Chapter 7
Understanding Bikeability: Insight into the Cycling-City Relationship Using Massive Dockless Bike-Sharing Records in Beijing

Enjia Zhang, Wanting Hsu, Ying Long, and Scott Hawken

Abstract Cycling records from emerging dockless bike-sharing services provide new opportunities to gain insight into the interactions between multiple fine-scale cycling characteristics and built environmental elements. Using Beijing as an example and the street as the analytic unit, this study examined the associations between three cycling characteristics and spatial visual elements while controlling for other built environmental features. The results showed that most visual elements were significantly associated with cycling characteristics, but their performance differs across models for trip distance, speed, and volume. The results also indicated that individuals riding long distances or at fast speeds preferred streets with more sky and greenery views. Likewise, wider streets with less spatial disorder, tended to have a higher riding volume. The findings can enhance the understanding of cycling behaviors and promote the implementation of urban design for more bikeable streets.

Keywords Dockless bike-sharing · Bikeability · Cycling characteristics · Spatial visual elements · Beijing

7.1 Introduction

Cycling is believed to promote the sustainable development of cities by providing a low-emission solution for commuting and recreational travel, especially in high-density cities where it can help address the last-mile problem (Nogal and Jimenez 2020). Additionally, it is considered a physical activity that brings health benefits

E. Zhang · W. Hsu · Y. Long (✉)
School of Architecture, Tsinghua University, Beijing, China
e-mail: ylong@tsinghua.edu.cn

E. Zhang
e-mail: zej18@mails.tsinghua.edu.cn

S. Hawken
School of Architecture and Civil Engineering, The University of Adelaide, Adelaide, Australia
e-mail: scott.hawken@adelaide.edu.au

R. Goodspeed et al. (eds.), *Intelligence for Future Cities*, The Urban Book Series,
https://doi.org/10.1007/978-3-031-31746-0_7

to individuals (Otero et al. 2018). Therefore, cycling behavior (Kaplan et al. 2015; Castanon & Ribeiro 2021) and influential elements from various aspects (Castanon & Ribeiro 2021; Hardinghaus et al. 2021; Shaer et al. 2021) have long been a topic of interest for scholars in transportation, urban planning, and public health (Forsyth & Krizek 2011; Hu et al. 2021; Li et al. 2021).

Benefiting from the development of information and communication technologies, docked and dockless IT-based bike-sharing, as emerging modes of cycling, have witnessed rapid growth recently (Pons et al. 2016; Chen et al. 2020). Meanwhile, IT-based bike-sharing can collect massive cycling records, enabling quantitative studies of the spatiotemporal behaviors and spatial preferences of cyclists. Previous studies have measured cycling behaviors and uncovered associated built environmental features, such as the density and distance of facilities, bike station attributes, geographic altitude, walkscore, street network, and mixed land use, based on the pick-up and drop-off data from bike stations (Faghih-Imani et al. 2014; El-Assi et al. 2017; Scott and Ciuro 2019).

Compared to bike-sharing based on docking stations, dockless bike-sharing allows users to pick up and drop off bicycles anywhere within a service zone (Orvin & Fatmi 2021). Dockless bike-sharing has the potential to effectively promote active travel, improve user mobility, encourage more users to participate in cycling (Orvin & Fatmi 2021), improve the efficiency of bicycle utilization (Tao & Zhou 2021), and extend the transfer radius of public transportation (Ai et al. 2019), in light of the delivered demand-responsive, multimodal services (Shaheen et al. 2012) and flexible access to public transportation (Duran-Rodas et al. 2020). Moreover, dockless shared bikes can collect more detailed and fine-scale cycling data for each street during a user's ride. Therefore, there has been a surge in research on the characteristics of dockless bike-sharing and its relationship with the built environment (Fan & Zheng 2020; Su et al. 2020; Li et al. 2021).

However, most studies have focused on cyclists' route choices, transfers with other public transportation, and bicycle parking, while failing to measure and compare other cycling characteristics, such as speed and distance. Furthermore, although some objective and perceived built environments, such as the distance to subway/bus stations, mixed land use, and the density of residential and office functions and buildings, have been shown to be highly associated with cycling trips (Scott & Ciuro 2019; Li et al. 2021; Guo & He 2021), the spatial visual elements in the streets (Goodspeed & Yan 2017) that urban designers and governments frequently highlight in urban design guidelines (Tang & Long 2019) have not been considered in these studies.

To address this research gap, this study used Beijing as a study area. The study analyses data from the bike-sharing company Mobike to portray three cycling characteristics, and compared their different relationships with spatial visual elements, while also controlling for other built environmental elements with the potential to influence cycling behaviors.

7.2 Methodology

7.2.1 Research Design

This study focused on the area within Beijing's Fifth Ring Road (667 km^2), which is the main urban built-up area for most commuter trips by all modes of transportation in Beijing. The analytic unit was a street segment, which is the portion of the road between two road intersections. Ordinary least squares (OLS) regression was used to examine the relationship between cycling characteristics and spatial visual elements. Meanwhile, we controlled for other built environmental factors that may influence travel demand (Ewing & Cervero 2010). Three cycling characteristics were examined in this study: average trip distance, average trip speed, and daily trip volume. Prior to regression analysis, data distribution was checked, and multicollinearity between independent variables and control variables was assessed (Fig. 7.1).

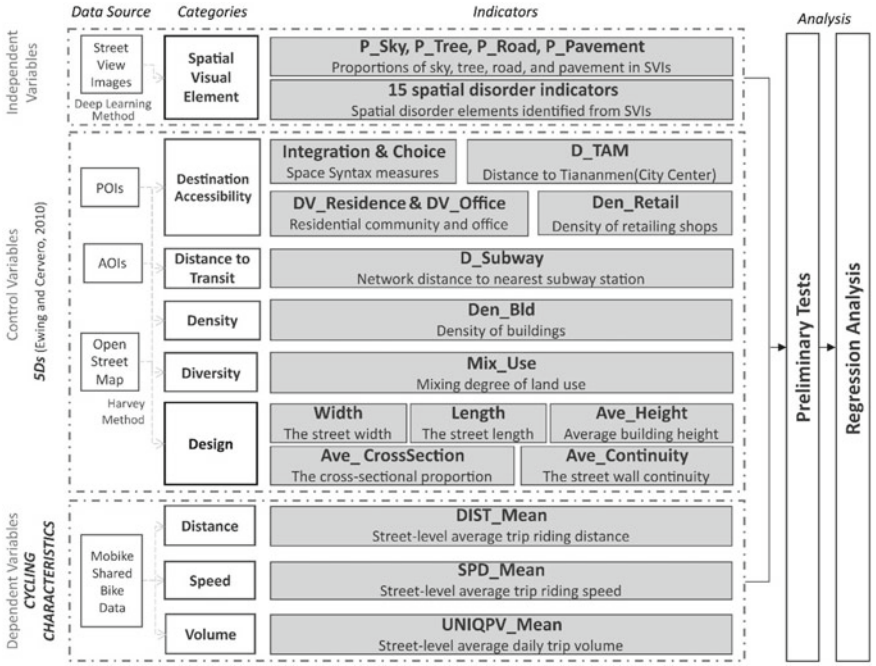

Fig. 7.1 Framework of this study

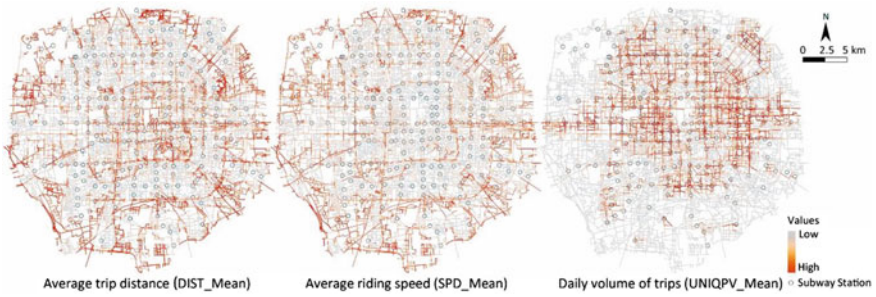

Fig. 7.2 Spatial visualization of three cycling characteristics using Jenks natural breaks

7.2.2 Variables and Data

7.2.2.1 Dependent Variable: Measurement of Cycling Characteristics

Dockless bike-sharing data were collected from Mobike, which was established in China in 2015 and quickly became one of the most popular bike-sharing companies. It was acquired by the e-commerce giant Meituan in April 2018. We collected anonymous bike trip records for the area within Beijing's Fifth Ring Road over a six-month period (181 days from January 1 to June 30, 2018), which were aggregated by street segment. The data included the street ID, date, daily user volume, daily bike trip volume, user's average speed, and average trip distance. Three indicators were calculated and used in this study: the average trip distance of all users who passed through a street segment (DIST_Mean), the average riding speed of all users who passed through a street segment (SPD_Mean), and the daily volume of Mobike trips on each street (UNIQPV_Mean), which were used to depict the distance, speed, and volume of cycling for each street. The data were anonymized to protect user privacy.

Figure 7.2 presents a spatial visualization of the three dependent variables. The average trip distances on the outer-ring streets were higher than those on the fourth-ring road and lower near subway stations. The spatial distribution of the average speed shared some commonalities with the previous map of average trip distances. The trip volume map showed that Mobike trips were concentrated in the city center and near subway stations. The differentiated patterns of these indicators indicate different associated built environmental elements.

7.2.2.2 Independent Variable: Measurement of Spatial Visual Elements

Spatial Visual Elements. The spatial visual elements considered as independent variables in this study were elements viewed from the street, which could be extracted from street-view images (SVI). We obtained the SVIs by crawling Tencent Map using its application programming interface (API). For all streets processed within the fifth ring road area, we divided each street segment into vertices with a distance

of 50 m, resulting in an average of four points for each street to collect SVIs that depict the overall visual conditions of each street regarding the continuity of street elements and landscape. The corresponding vertex coordinates were inputted into the place ID retrieval API and the API for downloading the SVIs of four horizontal angles: front, back, left, and right. As a result, several vertices spaced 50 m apart were distributed along the street for each street, providing us with 4-direction scenes for each vertex that may represent the overall spatial elements of a specific street.

Based on the SVIs, we used the SegNet pixel-wise image semantic segmentation method (Badrinarayanan et al. 2017) to calculate the proportions of the sky (P_Sky), trees (P_Tree), road (P_Road), and pavement (P_Pavement) to depict the streets' beauty (greenery and openness) and convivence for riding (road and pavement). Additionally, we measured 15 disorder indicators that could influence the perceived safety for cyclists (Kyttä et al. 2014) by applying the deep learning model proposed by Chen et al. (2022). Specifically, the 15 disorder indicators were abandoned buildings (Bld_Abandoned), buildings with damaged facades (BldFac_Damaged), buildings with unkempt facades (BldFac_Unkempt), graffiti/illegal advertisements (Adver_Graffiti), illegal/temporary buildings (Bld_Illegal), stores with poor signboards (Store_Poorsign), stores with poor facades (Store_Poorfac), vacant and pending stores (Store_Vacant), messy and unmaintained greening (Unmaingreen_Messy), garbage/litter on the street (Garbage), construction fence remnants (Fence_Remnant), broken roads (Road_Broken), occupied roads (Road_Occupied), broken infrastructure (Infra_Broken), and damaged public interfaces (Interface_Damaged). For each observed SVI point, we scored the presence of the above elements as 1; otherwise, it was 0. Thus, for each street, the average score for each disorder variable reflected the average degree of disorder.

7.2.2.3 Control Variable: Measurement of Five Ds

The five Ds (Destination Accessibility, Distance to Transit, Density, Diversity, and Design) have been identified as influential built environments that can moderate travel demands (Ewing & Cervero 2010). Therefore, this study introduced five Ds as control variables to better reveal the relationships between spatial visual indicators and cycling characteristics. Table 7.1 shows the descriptions of all variables.

Destination Accessibility. As the origin–destination is the primary determinant of the cycling route, two space syntax indicators were utilized to control the role of the street network in influencing the route preferences of cyclists: (1) the integration index, which gauges a street segment's ability to attract incoming traffic and reflects its centrality within the entire system, and (2) the choice index, which evaluates the benefits of a spatial unit as the shortest travel path and reflects the possibility of a street segment being traversed (Hillier 1999). We computed the integration and choice measures using analysis radii of 800 m (Int800, Cho800), 1600 m (Int1600, Cho1600), 2400 m (Int2400, Cho2400), 3200 m (Int3200, Cho3200), 4800 m (Int4800, Cho4800), 9600 m (Int9600, Cho9600), and n (global analysis, Intall, Choall), respectively. To evaluate access to the city center, we calculated the

Table 7.1 Descriptions of all variables (N = 16,266)

Variables	Indicator categories	Variables	Descriptions and methods	Mean	Std_Deviation	Unit
Dependent variables	Cycling characteristics	DIST_Mean	The average trip distance of all the users that passed through a street segment	4.3869	1.4587	km
		SPD_Mean	The average riding speed of all the users that passed through a street segment	10.2943	1.1337	km/h
		UNIQPV_Mean	The daily volume of Mobike trips on each street	173.4124	181.4656	#
Independent variables	Spatial visual elements	P_Sky	The average street-level proportions of the sky, trees, road, and pavement in all SVIs within the same street	0.1633	0.0930	–
		P_Tree		0.1948	0.1287	–
		P_Road		0.1540	0.0691	–
		P_Pavement		0.0843	0.0478	–
		Bld_Abandoned	The average score of identified spatial disorder elements in SVIs using MobileNet V3-small based on the results of Chen et al.'s (2022) within the same street	0.0042	0.0246	–
		BldFac_Damaged		0.0699	0.1163	–
		BldFac_Unkempt		0.0486	0.1037	–
		Adver_Graffiti		0.3661	0.2649	–
		Bld_Illegal		0.0097	0.0366	–
		Store_Poorsign		0.4853	0.2390	–
		Store_Poorfac		0.0536	0.0885	–
		Store_Vacant		0.0377	0.0751	–
		Unmaingreen_Messy		0.0179	0.0624	–
		Garbage		0.3250	0.2368	–
		Fence_Remnant		0.0840	0.1386	–

(continued)

Table 7.1 (continued)

Variables	Indicator categories	Variables	Descriptions and methods	Mean	Std_Deviation	Unit
		Road_Broken		0.2535	0.2366	–
		Road_Occupied		0.0492	0.1015	–
		Infra_Broken		0.1295	0.1922	–
		Interface_Damaged		0.1176	0.1706	–
Control Variables	Destination accessibility	Integration (Int800, Int1600, Int2400, Int3200, Int4800, Int9600, Intall)	Integration index value using space syntax analysis with analysis radius of 800 m, 1600 m, 2400 m, 3200 m, 4800 m, 9600 m, and n (global)	–	–	–
		Choice (Cho800, Cho1600, Cho2400, Cho3200, Cho4800, Cho9600, Choall)	Choice index value using space syntax analysis with analysis radius of 800 m, 1600 m, 2400 m, 3200 m, 4800 m, 9600 m, and n (global)	–	–	–
		D_TAM	The Euclidean distance to Tiananmen Square	8.6852	3.6139	km
		DV_Residence	Dummy variable: when the street is near residential communities (within 100 m), the score is 1, otherwise 0	0.7200	0.4500	–
		DV_Office	Dummy variable: when the street is near offices (within 100 m), the score is 1, otherwise 0	0.4000	0.4890	–

(continued)

Table 7.1 (continued)

Variables	Indicator categories	Variables	Descriptions and methods	Mean	Std_Deviation	Unit
		Den_Retail	The density of POIs of retail stores within each street's 50-m buffer	375.7777	636.824	#/km^2
	Distance to transit	D_Subway	The network distance to the nearest subway station	0.9811	0.8598	km
	Density	Den_Bld	The average number of buildings on two sides of a street	22.9867	16.8490	#/km^2
	Diversity	Mix_Use	The mixing degree of POIs using Shannon's entropy	0.5344	0.1998	–
	Design	Width	Distance between edges across the street	35.3800	18.7200	m
		Length	Centerline distance along a street	248.6848	179.9437	m
		Ave_Height	Average building height along the street	11.8000	14.5330	m
		Ave_CrossSection	Width/average height on both sides of the street	0.3766	0.5571	–
		Ave_Continuity	The average proportion of edge intersecting buildings on both sides of the street	0.3345	0.2325	–

Note We collected road networks, building footprints, AOI, and POI from Gaode map (https://lbs.amap.com) from its open API

distance from the midpoint of each street to the flag point base in Tiananmen Square (D_TAM). We also considered several crucial sites that could be potential origins or destinations for the rides, including dummy variables for residential communities (DV_Residence) and offices (DV_Office) within a 100-m distance to the street in the Area of Interest (AOI) data, and the density of retail stores (shopping and catering) within a 50-m buffer of the street (Den_Retail).

Distance to Transit. The network distance from the street segment to the nearest subway station (D_Subway) was regarded as the distance to transit.

Density. Density indicators were measured as building counts divided by the street length (Den_Bld).

Diversity. Diversity measures the mixing degree of land use in 50-buffer streets (Mix-Use). The normalized proportion of each main category of Point of Interest (POI) was calculated using Shannon's entropy.

Design. Some street-level urban forms in the design category, such as the width (Width) and length (Length) of the street, average height (Ave_Height) and continuity (Ave_Continuity) of surrounding buildings, and the average cross-section (street width/building height) (Ave_CrossSection) were also calculated by referring to the GIS-based methods developed by Harvey (2014).

7.3 Results

7.3.1 Data Processing and Preliminary Tests

Before conducting the regression analysis, we checked the distributions of all variables. Since Den_Retail and UNIQPV_Mean were long-tailed data, we used the log transformation on these two variables to ensure the reliability of the models. Then, we applied Pearson's correlation and variance inflation factor (VIF) tests to avoid the multicollinearity effect. The results showed that the multicollinearity of the model was not severe, with Pearson's correlation coefficients less than 0.8, and VIF values less than 5.

To ensure that the OLS model performed better, we calculated the Pearson correlations between the various space syntax measures and the three cycling characteristic indicators. We selected those with higher coefficients to be used in the following regression analysis. The results showed that for DIST_Mean, Int800 and ChoAll had the highest values; for SPD_Mean, Int1600 and Cho800 showed a closer relationship; and for LnUNIQPV_Mean, Int3200 and Cho3200 presented the highest coefficients. Therefore, this study considered different integration and choice variables in the three regression models.

7.3.2 Regression Analysis and Results

Table 7.2 displays the results of the regression models with different dependent variables. The results showed that the built environmental variables could explain 41.2% of the trip distance, 34.8% of the cycling speed, and 54.9% of the trip volume, suggesting that trip volume has a stronger relationship with built environmental elements than trip speed and distance.

Among all the spatial visual variables, the proportions of roads and pavements in the SVIs were significantly associated with all three cycling characteristics, while most indicators such as P_Sky, P_Tree, Bld_Abandoned, BldFac_Unkempt, Adver_Graffiti, Bld_Illegal, Store_Poorsign, Store_Poorfac, Unmaingreen_Messy, Garbage, Road_Broken, and Road_Occupied, were only relevant to cycling characteristics in specific contexts.

The results revealed that people preferred to ride at a faster speed on streets with broader views of sky, greenery, roads, and pavements, as all the proportions of sky, trees, road, and pavement in the SVIs were significantly positive with trip distance and cycling speed. For trip volume, the proportion of roads had a positive correlation, but the pavement proportion had adverse effects. This implies that wider roads with narrower sidewalks were more likely to witness more bike-sharing trips.

The findings for the spatial disorder indicators showed that different cycling characteristics were related to diverse elements. Long-distance rides usually occurred in areas with poor spatial quality, such as abandoned buildings, unkempt building façades, poor store façades, and broken roads. This implies that people who lived near urban villages (usually with poor spatial quality) tended to use shared bikes for long-distance commuting.

The results for speed suggested that people would quickly pass places with garbage and slow down along streets with unkempt illegal/temporary buildings and messy and unmaintained greening. One possible explanation is that places with poor greenery and temporary buildings are usually commercial or residential in suburban areas, which could be destinations for riders.

As for trip volumes, some small elements, such as Adver_Graffiti, Store_Poorsign, and Garbage, had positive coefficients, whereas some larger items, such as unkempt buildings, messy and unmaintained greenery and busy car-filled roads, were negatively associated. This implies that disorder in buildings, landscapes, and roads could hinder people's path choices for cycling.

Figure 7.3 presents the standardized coefficients for the significant indicators, allowing for a more direct interpretation of the differences in the regression results among different cycling characteristics. The results showed that street network features, potential origin and destination places, access to subway stations, mixed land use, and some urban form indicators were highly associated with cycling characteristics, which is consistent with previous studies (Guo & He 2021; Zhuang et al. 2022). The results also suggest that visual elements on the street, such as the proportion of sky, trees, roads, and pavement, are much more critical for riders than spatial disorder indicators on the two sides of the street. Moreover, more spatial disorder

Table 7.2 Comparison between results using different cycling behaviors as dependent variables

N = 16,266	Variable description	DIST_Mean	SPD_Mean	LnUNIQPV_Mean
Destination accessibility	Int800	−1.446[c] (0.421)		
	Int1600		−1.198[c] (0.190)	
	Int3200			2.097[c] (0.090)
	Cho800		−0.036[b] (0.014)	
	Cho3200			0.000 (0.000)
	ChoAll	0.000[c] (0.000)		
	D_TAM	−0.082[c] (0.003)	0.011[c] (0.003)	−0.011[c] (0.003)
	DV_Residential	−0.501[c] (0.019)	−0.319[c] (0.019)	0.517[c] (0.019)
	DV_Office	0.048[b] (0.017)	0.202[c] (0.016)	0.168[c] (0.017)
	LnDen_Retail	0.008 (0.004)	−0.011[a] (0.004)	0.051[c] (0.005)
Distance to transit	D_Subway	0.400[c] (0.011)	0.171[c] (0.011)	−0.316[c] (0.011)
Density	Den_Bld	−0.004[c] (0.001)	−0.007[c] (0.001)	−0.007[c] (0.001)
Diversity	Mix_Use	−1.248[c] (0.065)	−1.195[c] (0.063)	1.820[c] (0.066)
Design	Width	−0.002[c] (0.000)	0.000 (0.000)	0.007[c] (0.000)
	Length	0.000[c] (0.000)	0.001[c] (0.000)	0.000[c] (0.000)
	Ave_Height	−0.002[a] (0.001)	0.001 (0.001)	−0.001[a] (0.001)
	Ave_Section	−0.100[c] (0.017)	−0.067[c] (0.016)	−0.057[c] (0.017)
	Ave_Continuity	−0.278[c] (0.053)	−0.154[a] (0.051)	−0.346[c] (0.053)
Spatial visual element	P_Sky	3.375c (0.136)	1.819[c] (0.130)	−0.005 (0.136)
	P_Tree	1.136[c] (0.074)	0.416[c] (0.071)	−0.144 (0.074)
	P_Road	1.072[c] (0.156)	0.867[c] (0.149)	2.871[c] (0.157)

(continued)

Table 7.2 (continued)

N = 16,266	Variable description	DIST_Mean	SPD_Mean	LnUNIQPV_Mean
	P_Pavement	1.845[c] (0.177)	0.490[b] (0.170)	−1.296[c] (0.178)
	Bld_Abandoned	0.646[a] (0.315)	0.290 (0.301)	−0.055 (0.317)
	BldFac_Damaged	−0.105 (0.077)	0.008 (0.074)	−0.114 (0.078)
	BldFac_Unkempt	0.420[c] (0.088)	0.094 (0.084)	−0.650[c] (0.089)
	Adver_Graffiti	−0.049 (0.029)	−0.043 (0.027)	0.192[c] (0.029)
	Bld_Illegal	−0.392 (0.216)	−0.548[b] (0.207)	0.104 (0.217)
	Store_Poorsign	−0.052 (0.031)	−0.016 (0.029)	0.161[c] (0.031)
	Store_Poorfac	0.342[c] (0.096)	−0.073 (0.092)	−0.176 (0.097)
	Store_Vacant	−0.189 (0.110)	−0.119 (0.105)	−0.006 (0.110)
	Unmaingreen_Messy	−0.185 (0.126)	−0.248[a] (0.120)	−0.598[c] (0.127)
	Garbage	0.059 (0.032)	0.068[a] (0.031)	0.107[c] (0.032)
	Fence_Remnant	0.051 (0.058)	−0.082 (0.055)	0.028 (0.058)
	Road_Broken	0.070[a] (0.032)	0.044 (0.031)	0.001 (0.032)
	Road_Occupied	−0.057 (0.082)	−0.042 (0.078)	−0.223[b] (0.082)
	Infra_Broken	−0.022 (0.046)	0.077 (0.044)	−0.013 (0.047)
	Interface_Damaged	0.034 (0.044)	−0.017 (0.043)	0.016 (0.045)
R^2		0.414	0.349	0.550
Adjusted R^2		0.412	0.348	0.549

Note The table reports the coefficients and predictive power (R^2) for each model's column. Standard errors are in parentheses. Significance level: [a]$p < 0.05$, [b]$p < 0.01$, and [c]$p < 0.001$

elements were associated with trip volume than with distance and speed, while more visual proportion indicators from the street view were significantly correlated with trip distance and speed than with volume. These results reflected riders' varying preferences for spatial visual elements.

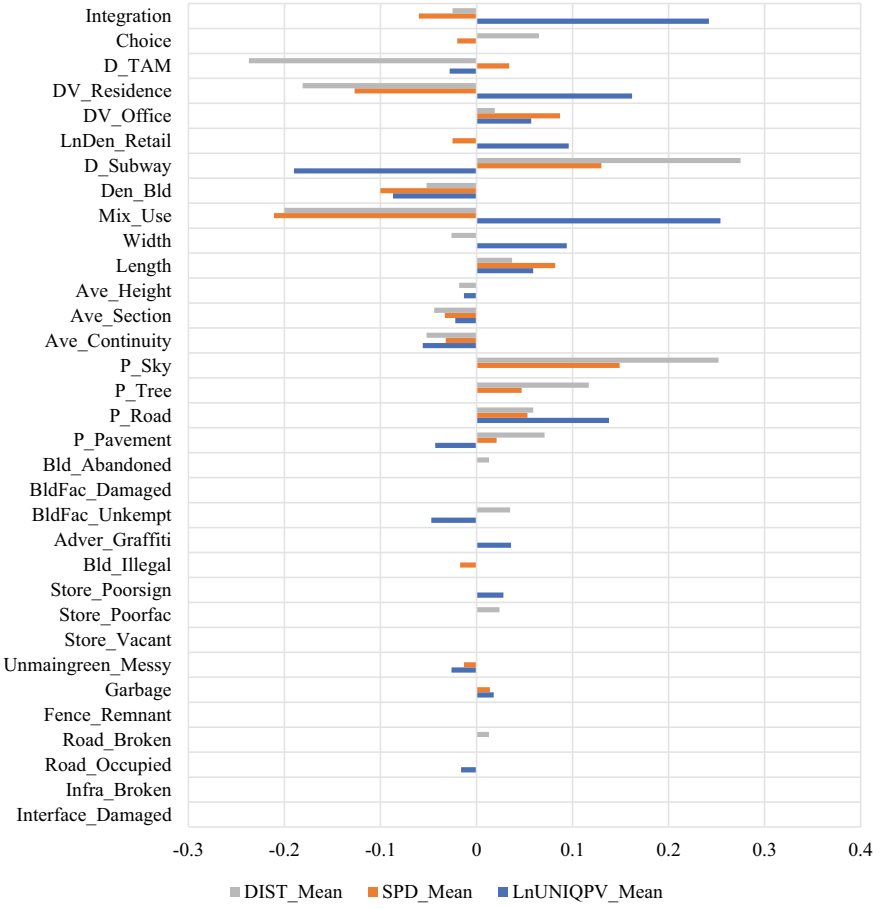

Fig. 7.3 Comparison between the standardized coefficients of statistically significant indicators ($p < 0.05$) for three cycling characteristics

7.4 Conclusions and Discussion

Taking Beijing's central city as the study area and street segments as the analytic unit, this study examined the relationship between three cycling characteristics (average trip distance, average riding speed, and daily volume) and spatial visual elements by controlling for other potentially influential built environmental factors. After controlling for the role of street segments in the whole road network and the width of the road, the results revealed that individuals who ride long distances or at high speeds preferred a broad vision of sky and trees on the streets, while wider streets with fewer spatial disorder elements in terms of larger items such as buildings, landscapes, and roads could have a higher riding volume. Moreover, the results suggested that the

visual proportions of elements on the road were much more critical for riders than spatial disorder indicators on both sides of the street.

The findings could enhance our understanding of cyclists' spatial preferences regarding different riding scenarios (e.g., long-distance riding, high-speed riding, most frequent riding) and promote urban design implementations for more bikeable streets. The results revealed distinct spatial visual elements for different cycling characteristics, which can help urban designers develop corresponding guidelines and encourage people to promote this sustainable commuting mode and improve the overall usage efficiency of the bike-sharing system.

However, there are still some limitations to be addressed in future research. First, due to the limitations of data acquisition, we could only obtain the data aggregated to the street segment, and not each ride's specific OD and path data. With more data, future studies could consider the route choice and direction of cycling to analyze the built environmental elements along the entire ride trip and on the closed side of the street. Second, further studies should expand the data sources to measure bike infrastructure, such as bike lanes and parking areas, to better investigate preferences for cycling and parking.

Funding This work was supported by the National Natural Science Foundation of China grant number 52178044 and the UNSW-TSINGHUA UNIVERSITY Collaborative Research Fund RG180121.

References

Ai Y, Li ZP, Gan M (2019) A solution to measure traveler's transfer tolerance for walking mode and dockless bike-sharing mode. J Supercomput 75(6):3140–3157

Badrinarayanan V, Kendall A, Cipolla R (2017) Segnet: a deep convolutional encoder-decoder architecture for image segmentation. IEEE Trans Pattern Anal Mach Intell 39(12):2481–2495

Castanon UN, Ribeiro PJG (2021) Bikeability and emerging phenomena in cycling: exploratory analysis and review. Sustainability 13(4):2394

Chen ZY, van Lierop D, Ettema D (2020) Dockless bike-sharing systems: what are the implications? Transp Rev 40(3):333–353

Chen J, Chen L, Li Y et al (2022) Measuring physical disorder in urban street spaces: a large-scale analysis using street view images and deep learning. Ann Am Assoc Geogr https://doi.org/10.1080/24694452.2022.2114417

Duran-Rodas D, Villeneuve D, Wulfhorst G (2020) Bike-sharing: the good, the bad, and the future -an analysis of the public discussion on twitter. Eur J Transp Infrastruct Res 20(4):38–58

El-Assi W, Mahmoud MS, Habib KN (2017) Effects of built environment and weather on bike sharing demand: a station level analysis of commercial bike sharing in Toronto. Transportation 44(3):589–613

Ewing R, Cervero R (2010) Travel and the built environment. J Am Plann Assoc 76(3):265–294

Faghih-Imani A, Eluru N, El-Geneidy AM et al (2014) How land-use and urban form impact bicycle flows: evidence from the bicycle-sharing system (BIXI) in Montreal. J Transp Geogr 41:306–314

Fan YC, Zheng SQ (2020) Dockless bike sharing alleviates road congestion by complementing subway travel: evidence from Beijing. Cities 107:102895

Forsyth A, Krizek K (2011) Urban design: is there a distinctive view from the bicycle? J Urban Des 16(4):531–549
Goodspeed R, Yan X (2017) Crowdsourcing street beauty: Visual preference surveys in the big data era. In: Schintler LA, Chen Z (eds) Big data for regional science. Routledge, London and New York, pp 75–93
Guo Y, He S (2021) The role of objective and perceived built environments in affecting dockless bike-sharing as a feeder mode choice of metro commuting. Transp Res Part A Policy Pract 149:377–396
Hardinghaus M, Nieland S, Lehne M et al (2021) More than bike lanes-a multifactorial index of urban bikeability. Sustainability 13(21):11584
Harvey CW (2014) Measuring streetscape design for livability using spatial data and methods. University of Vermont, Vermont
Hillier B (1999) Space is the machine: a configurational theory of architecture. Cambridge University Press, Cambridge
Hu SH, Xiong CF, Liu ZQ et al (2021) Examining spatiotemporal changing patterns of bike-sharing usage during Covid-19 pandemic. J Transp Geogr 91:102997
Kaplan S, Manca F, Nielsen TAS et al (2015) Intentions to use bike-sharing for holiday cycling: an application of the theory of planned behavior. Tour Manag 47:34–46
Kyttä M, Kuoppa J, Hirvonen J et al (2014) Perceived safety of the retrofit neighborhood: a location-based approach. Urban Des Int 19(4):311–328
Li HW, Xing YY, Zhang WB et al (2021) Investigating the impact of weather conditions and land use on dockless bike-share trips in Shanghai, China. J Urban Plann Dev 147(4):237688371
Nogal M, Jimenez P (2020) Attractiveness of bike-sharing stations from a multi-modal perspective: the role of objective and subjective features. Sustainability 12(21):9062
Orvin MM, Fatmi MR (2021) Why individuals choose dockless bike sharing services? Travel Behav Soc 22:199–206
Otero I, Nieuwenhuijsen MJ, Rojas-Rueda D (2018) Health impacts of bike sharing systems in Europe. Environ Int 115:387–394
Pons, JMS Llado JM, Perez MR et al (2016) Bike-sharing schemes and sustainable urban mobility. An analysis in the city of Palma (Mallorca, Balearic Islands). Boletin de la Asoc de Geogr Espanoles 71:227−245
Scott DM, Ciuro C (2019) What factors influence bike share ridership? an investigation of hamilton, Ontario's bike share hubs. Travel Behav Soc 16:50–58
Shaer A, Rezaei M, Rahimi BM et al (2021) Examining the associations between perceived built environment and active travel, before and after the covid-19 outbreak in Shiraz city. Iran Cities 115:103255
Shaheen S, Guzman S, Zhang H (2012) Bikesharing across the globe. In: City cycling. MIT Press, UC Berkeley: Transportation Sustainability Research Center, p 183.
Su D, Wang YC, Yang N et al (2020) Promoting considerate parking behavior in dockless bike-sharing: an experimental study. Transp Res Part A Policy Pract 140:153–165
Tang J, Long Y (2019) Measuring visual quality of street space and its temporal variation: methodology and its application in the hutong area in Beijing. Landsc Urban Plan 191:103436
Tao J, Zhou ZH (2021) Evaluation of potential contribution of dockless bike-sharing service to sustainable and efficient urban mobility in China. Sustain Prod Consum 27:921–932
Zhuang C, Li S, Tan Z et al (2022) Nonlinear and threshold effects of traffic condition and built environment on dockless bike sharing at street level. J Transp Geogr 102:103375